Ionic Dispersion of Pt over CeO_2 by the Combustion Method: Structural Investigation by XRD, TEM, XPS, and EXAFS

Parthasarathi Bera,[†] K. R. Priolkar,[‡] Arup Gayen,[†] P. R. Sarode,[‡] M. S. Hegde,*[,†] S. Emura,[§] R. Kumashiro,[||] V. Jayaram,[†] and G. N. Subbanna[⊥]

Solid State and Structural Chemistry Unit, Indian Institute of Science, Bangalore 560012, India, Department of Physics, Goa University, Goa 403206, India, Institute of Scientific and Industrial Research, Osaka University, Mihoga-oka 8-1, Ibaraki, Osaka 567-0047, Japan, Department of Material Science, Faculty of Science, Osaka City University, Sugimoto 3-3-138, Sumiyoshi-ku, Osaka 558-8585, Japan, and Materials Research Centre, Indian Institute of Science, Bangalore-560012, India

Received December 10, 2002. Revised Manuscript Received March 14, 2003

The structure and chemical nature of Pt in combustion-synthesized Pt/CeO_2 catalysts have been investigated by X-ray diffraction (XRD), transmission electron microscopy (TEM), X-ray photoelectron spectroscopy (XPS), extended X-ray absorption fine structure (EXAFS), and temperature-programmed reaction (TPR). Catalytic oxidation of CO over Pt/CeO_2 is correlated with its structure. High-resolution XRD studies show that the structure could be refined for the composition of $Ce_{1-x}Pt_xO_{2-\delta}$ in the fluorite structure with 6% oxide ion vacancy. TEM images show very few Pt particles on the CeO_2 crystallite surface in as-prepared samples and a decrease in the density of Pt metal particles is observed on heating. XPS studies demonstrate that Pt is dispersed mostly in +2 (72%) and +4 (21%) oxidation states on CeO_2, whereas only 7% is present as Pt metal particles. On heat treatment, Pt^{2+} species increase at the cost of Pt^{4+} ions. EXAFS studies show the average coordination number of 1.3 around the platinum ion in the first shell of 1% Pt/CeO_2 at a distance of 1.98 Å, indicating oxide ion vacancy around the platinum ion. On heating, the average oxygen coordination of Pt and oxygen increases to 2.3. The second shell at 2.97 Å is due to Pt−Pt coordination, which is absent in PtO_2 and PtO. The third shell at 3.28 Å is not observed either in Pt metal or any of the platinum oxides, which could be attributed to Pt^{2+}−Ce^{4+} correlation. Thus, Pt/CeO_2 forms a $Ce_{1-x}Pt_xO_{2-\delta}$ type of solid solution having $-\square-Pt^{2+}-O-Ce^{4+}-$ kinds of linkages.

Introduction

Studies on the structure, active species, and properties of supported metal catalysts have found great interest in heterogeneous catalysis for many years.[1−8] The catalytic activity of dispersed metal catalyst is influenced by many factors such as relative amount of metals present, extent of dispersion, heat treatment, method of preparation, chemical nature of support, and strength of metal−support interaction. Understanding of chemical phenomena due to heat treatment of these catalysts is of fundamental interest because thermal treatment can influence the morphology, stability, chemical nature, and activity of supported metal catalysts. Previous investigations on thermal behavior have mainly focused on the metal catalysts dispersed on silica, alumina, magnesia, carbon, and zeolite supports.[9−16] These catalysts are commonly prepared by impregnation, ion exchange, coprecipitation, and deposi-

* Corresponding author. E-mail: mshegde@sscu.iisc.ernet.in. Fax: +91-80-3601310.
[†] Solid State and Structural Chemistry Unit, Indian Institute of Science.
[‡] Goa University.
[§] Osaka University.
[||] Osaka City University.
[⊥] Materials Research Centre, Indian Institute of Science.
[#] E-mail: partho@sscu.iisc.ernet.in.

(1) Augustine, R. L. In *Heterogeneous Catalysis for the Synthetic Chemist*; Marcel Dekker: New York, 1996; p. 153.
(2) Jin, T.; Zhou, Y.; Mains, G. J.; White, J. M. *J. Phys. Chem.* **1987**, *91*, 5931.
(3) Rainer, D. R.; Koranne, M.; Vesecky, S. M.; Goodman, D. W. *J. Phys. Chem. B* **1997**, *101*, 10769.
(4) Martínez-Arias, A.; Coronado, J. M.; Cataluña, R.; Conesa, J. C.; Soria, J. *J. Phys. Chem. B* **1998**, *102*, 4357.
(5) Blanco, G.; Calvino, J. J.; Cauqui, M. A.; Corchado, P.; López-Cartes, C.; Colliex, C.; Pérez-Omil, J. A.; Stephan, O. *Chem. Mater.* **1999**, *11*, 3610.
(6) Harrison, P. G.; Bailey, C.; Daniell, W.; Zhao, D.; Ball, I. K.; Goldfarb, D.; Lloyd, N. C.; Azelee, W. *Chem. Mater.* **1999**, *11*, 3643.
(7) Harrison, P. G.; Ball, I. K.; Azelee, W.; Daniell, W.; Goldfarb, D. *Chem. Mater.* **2000**, *12*, 3715.
(8) Kulyova, S. P.; Lunina, E. V.; Lunin, V. V.; Kostyuk, B. G.; Muravyova, G. P.; Kharlanov, A. N.; Zhilinskaya, E. A.; Aboukaïs, A. *Chem. Mater.* **2001**, *13*, 1491.
(9) Toupance, T.; Kermarec, M.; Louis, C. *J. Phys. Chem. B* **2000**, *104*, 965.
(10) Stencel, J. M.; Diehl, J. R.; D'Este, J. R.; Makovsky, L. F.; Rodrigo, L.; Marcinkowska, K.; Adnot, A.; Roberge, P. C.; Kaliaguine, S. *J. Phys. Chem.* **1986**, *90*, 4739.
(11) Castner, D. G.; Watson, P. R.; Chan, I. Y. *J. Phys. Chem.* **1989**, *93*, 3188.
(12) Hoffmann, D. P.; Proctor, A.; Houalla, M.; Hercules, D. M. *J. Phys. Chem.* **1991**, *95*, 5552.
(13) Ballinger, T. H.; Yates, J. T., Jr. *J. Phys. Chem.* **1991**, *95*, 1694.
(14) Purnell, S. K.; Sanchez, K. M.; Patrini, R.; Chang, J.-R.; Gates, B. C. *J. Phys. Chem.* **1994**, *98*, 1205.
(15) Chen, A. A.; Vannice, M. A.; Phillips, J. *J. Phys. Chem.* **1987**, *91*, 6257.
(16) Boyanov, B. I.; Morrison, T. I. *J. Phys. Chem.* **1996**, *100*, 16310.

10.1021/cm0204775 CCC: $25.00
Published on Web 04/24/2003

tion methods. Chen et al.[17] have shown the diffusion of Rh from the top surface layer to bulk Al_2O_3 upon heating Rh/Al_2O_3 at 825 °C. Louis et al.[18] have reported the growth of Ni metal particles during thermal treatment of Ni/SiO_2 catalyst. Recently, Harrison et al. have reported thermal treatment studies on the nature of Cu and Cr species over SnO_2 and CeO_2 supports.[19−21]

Noble metals such as Pt and Pd dispersed on CeO_2 are widely used in automobile exhaust emission control due to oxygen storage capacity (OSC), higher dispersion of metals, and their promoting action.[22−27] Therefore, structure of CeO_2 supported noble metal catalysts is of great interest in autoexhaust catalysis. Recently, we reported[28] combustion-synthesized Pt/CeO_2 and Pd/CeO_2 catalysts which are active for NO reduction and CO and hydrocarbon oxidation. It has been observed that Pt/CeO_2 catalyst is more active than Pt/Al_2O_3 prepared by the same method. Pt/CeO_2 is also active for partial oxidation of CH_4 into $CO + 2H_2$ without formation of platinum carbide phase, even when reaction was carried out at 800 °C for 100 h.[29] However, the exact electronic as well as atomic structure of the Pt/CeO_2 system is not yet fully characterized to explain the active state of Pt on CeO_2. Further, any variation of Pt species on CeO_2 as a function of temperature has not been reported in the literature.

Generally, it is believed that Pt^0 is the active site in the dispersed Pt catalysts because Pt metal particles of 2−7 nm in size are finely dispersed over supports such as Al_2O_3, SiO_2, and ZrO_2. Unlike SiO_2 and Al_2O_3, CeO_2 is a reducible oxide support and, therefore, noble metals such as Pt and Pd can become oxidized over this kind of support. In the present investigation, Pt/CeO_2 catalysts of different concentrations prepared by a novel solution combustion method have been studied for their structure and catalytic properties. These catalysts were subjected to thermal treatment at 800 °C for 100 h to understand the dispersion, chemical nature, and thermal stability of the catalysts. Catalytic activity of combustion-synthesized Pt/CeO_2 is also compared with nano Pt metal particles as well as Pt/CeO_2 prepared by dispersing Pt over CeO_2. The structural characterization of as-prepared as well as heat-treated Pt/CeO_2 catalysts and other related catalysts have been carried out by several physical techniques including XRD, TEM, XPS, EXAFS, and TPR. It has been shown that $Ce_{1-x}Pt_xO_{2-\delta}$ type of solid solution is formed in the combustion-synthesized Pt/CeO_2 catalyst and the concentration of Pt^{2+} component increases upon heat treatment.

Experimental Section

Synthesis. Pt/CeO_2 catalysts were synthesized by the solution combustion method. For example, the combustion mixture for the preparation of 1% Pt/CeO_2 contained $(NH_4)_2Ce(NO_3)_6$, H_2PtCl_6, and $C_2H_6N_4O_2$ (oxalyldihydrazide) in the mole ratio 0.99:0.01:2.38. Oxalyldihydrazide (ODH) prepared from diethyl oxalate and hydrazine hydrate was used as the fuel. In a typical preparation, 10 g of $(NH_4)_2Ce(NO_3)_6$ (E. Merck India Ltd., 99.9%), 0.095 g of H_2PtCl_6 (Ranbaxy Laboratories Ltd., 99%), and 5.175 g of ODH were dissolved in 30 cm^3 of water in a borosilicate dish of 300 cm^3 capacity. The dish containing the redox mixture was introduced into a muffle furnace maintained at 350 °C. Initially, the solution boiled with frothing and foaming and underwent dehydration. At the point of complete dehydration, the surface ignited, burning with a flame (∼1000 °C) and yielding a voluminous solid product within 5 min. Similarly, 2−5% Pt/CeO_2 catalysts were prepared by the same method. The as-prepared Pt/CeO_2 samples were heated at 800 °C for 100 h in air.

To compare the structure and catalytic activity of combustion-synthesized 2% Pt/CeO_2 with the same catalyst prepared by another method, 2 at. % Pt was dispersed over combustion-synthesized CeO_2 by reducing H_2PtCl_6 solution with hydrazine hydrate. The solid was washed thoroughly with distilled water and ethanol and dried at 100 °C for 12 h. The catalyst is called 2% Pt/CeO_2 (dispersed). To see whether Pt metal can be oxidized over CeO_2, Pt/CeO_2 (dispersed) was heated in air as well as in an evacuated (∼10^{-5} Torr) sealed tube at 800 °C for 24 h. Fine Pt metal particles were also prepared by the polyol method to show the difference in catalytic activity with combustion-synthesized 2% Pt/CeO_2. H_2PtCl_6 was reduced in ethylene glycol solution at 180 °C, giving Pt particles of 6−7 nm as seen from TEM studies.

Catalytic Test. CO oxidation by O_2 over these materials was carried out in a TPR system equipped with a quadrupole mass spectrometer QXK300 (V G Scientific Ltd., England) for product analysis in a packed bed tubular quartz reactor of 250-mm length and 4 mm internal diameter at atmospheric pressure. Typically, 150 mg of each catalyst (40/80 mesh) diluted with 50 mg of SiO_2 (30/60 mesh) was loaded in the reactor with its endings plugged with ceramic wool. It must be noted that 3.4 mg of Pt is present in 150 mg of 2% Pt/CeO_2 catalyst and the same amount of Pt metal particles diluted with SiO_2 was taken in our experiment. The sample temperature was measured by a fine chromel−alumel thermocouple immersed in the catalyst bed. The gas flow was controlled using mass flow sensors (Bronkhorst Hi-Tech BV) calibrated against a standard bubble flowmeter. Before the catalytic test, the catalyst was heated in oxygen at 500 °C for 1 h followed by degassing in He flow to room temperature. Then the He flow was replaced with reactant flow having an inlet gas composition of CO (2 vol.%) and O_2 (1 vol.%) with He as balance, keeping total flow at 100 sccm to achieve a gas hourly space velocity (GHSV) of 43000 h^{-1}. All reactions were carried out as a function of temperature with a linear heating rate of 10 °C min^{-1}. The gaseous products were sampled through a fine control leak valve to an ultrahigh vacuum (UHV) system housing the quadrupole mass spectrometer at 10^{-9} Torr. Final pressure of the gases in the vacuum system was 2×10^{-5} Torr. All the masses were scanned in every 10 s. At the end of the reaction, the intensity of each mass as a function of temperature (thermogram) was generated. A gas mixture of 5% O_2 in He and CO were obtained from Bhoruka Gases Ltd., Bangalore. The purity of the gas mixture and CO was 99.95%.

Characterization. High-resolution XRD data for Rietveld analysis were collected in a Rigaku-2000 diffractometer with a rotating anode using Cu Kα radiation with a graphite-crystal monochromator to filter Kβ lines. Data were obtained at a scan rate of 1° min^{-1} with 0.02° step size in the 2θ range 10−110° and the structure was refined using the FullProf-98 program. The number of parameters refined simultaneously was 19.

TEM of the powders of these materials was carried out using a JEOL JEM-200CX transmission electron microscope operated at 200 kV.

(17) Chen, J. G.; Colaianni, M. L.; Chen, P. J.; Yates, J. T., Jr.; Fisher, G. B. *J. Phys. Chem.* **1990**, *94*, 5059.
(18) Louis, C.; Cheng, Z. X.; Che, M. *J. Phys. Chem.* **1993**, *97*, 5703.
(19) Harrison, P. G.; Lloyd, N. C.; Daniell, W. *J. Phys. Chem. B* **1998**, *102*, 10672.
(20) Harrison, P. G.; Daniell, W. *Chem. Mater.* **2001**, *13*, 1708.
(21) Harrison, P. G.; Allison, F. J.; Daniell, W. *Chem. Mater.* **2002**, *14*, 499.
(22) Taylor, K. C. *Catal. Rev.−Sci. Eng.* **1993**, *35*, 457.
(23) Kummer, J. T. *J. Phys. Chem.* **1986**, *90*, 4747.
(24) Yao, H. C.; Yao, Y.-F. Yu *J. Catal.* **1984**, *86*, 254.
(25) Oh, S. H. *J. Catal.* **1990**, *124*, 477.
(26) Nunan, J. G.; Robota, H. J.; Cohn, M. J.; Bradley, S. A. *J. Catal.* **1992**, *133*, 309.
(27) de Leitenburg, C.; Trovarelli, A.; Zamar, F.; Maschio, S.; Dolcetti, G.; Llorca, J. *J. Chem. Soc., Chem. Commun.* **1995**, 2181.
(28) Bera, P.; Patil, K. C.; Jayaram, V.; Subbanna, G. N.; Hegde, M. S. *J. Catal.* **2000**, *196*, 293.
(29) Pino, L.; Recupero, V.; Beninati, S.; Shukla, A. K.; Hegde, M. S.; Bera, P. *Appl. Catal. A* **2002**, *225*, 63.

XPS of these materials was recorded in an ESCA-3 Mark II spectrometer (V G Scientific Ltd., England) using Al Kα radiation (1486.6 eV). Binding energies were calculated with respect to C(1s) at 285 eV and were measured with a precision of 0.2 eV. For XPS analysis, the powder samples were made into pellets of 8 mm diameter and placed into an ultrahigh vacuum (UHV) chamber at 10^{-9} Torr housing the analyzer. The experimental data were curve-fitted with Gaussian peaks after subtracting a linear background. The concentrations of different states were estimated from the area of the respective Gaussian peaks.

EXAFS spectra of Pt L_{III}-edge in combustion-synthesized catalysts and reference samples were recorded at room temperature both in transmission mode and in fluorescence mode by using synchrotron radiation, employing a Si(111) double-crystal monochromator at BL01B1 beamline in Japan Synchrotron Radiation Research Institute (SPring-8), Japan. The first mirror and the monochromator were fully tuned to obtain optimal resolution. The slit width of the monochromator exit was 0.3 mm vertical and 6 mm horizontal to ensure a good signal to noise ratio. During the measurement the synchrotron was operated at an energy of 8 GeV and a current between 80 and 100 mA. The spectra were scanned in the range 11200−12500 eV for the Pt L_{III}-edge EXAFS. The photon energy was calibrated for each scan with the first inflection point of Pt L_{III}-edge in Pt metal foil (11561 eV). Both the incident (I_o) and transmitted (I) synchrotron beam intensities were measured simultaneously using ionization chambers filled with a mixture of 15% Ar and 85% N_2 gases and 100% Ar gas, respectively. The absorbers were made by pressing the samples into pellets of 10 mm diameter with boron nitride as the binder. The thickness of the absorber was adjusted such that $\Delta\mu_o x$ was restricted to a value ≤ 1, where $\Delta\mu_o$ is the edge step in the absorption coefficient and x is the sample thickness.[30] For 1% Pt/CeO_2 samples the fluorescence mode of detection was employed. In this mode a Lytle detector with 100% Kr gas was used to measure the reflected intensity. A Ge filter was used to filter the fluorescence lines in the Pt L_{III}-edge EXAFS region. The absorber was prepared by sprinkling fine powder of the sample uniformly on a Kapton tape and stacking a number of such layers together to achieve a desired thickness.

EXAFS Data Analysis. EXAFS data have been analyzed using the UWXAFS program.[31] It uses the criteria of good background removal, optimization of the low R portion of the EXAFS data, and Fourier transform to R space. Since the EXAFS function is a superposition of an unknown number of coordination shells, the Fourier transform (FT) technique gives information about the individual shells. Here, FT of the EXAFS function $\chi(k)$ to R space with a k^3 weighting factor and Hanning window function (Dk1 and Dk2 = 0.1) has been performed in 3−12 $Å^{-1}$, yielding a function $\Phi(R)$. The function $\Phi(R)$, where R is the distance from the absorber atom, is called a radial distribution function (RDF) or radial structure function (RSF). The value of amplitude reduction factor (S_o^2) is deduced from Pt L_{III}-edge EXAFS of Pt metal with known crystal structural data.[32] The theoretical calculation of back-scattering amplitude and phase shift functions are obtained by using the FEFF (6.01) program.[33] The input files for the FEFF program are directly given from crystal structure information of atoms such as lattice parameters, space group, and absorbing core. The experimental EXAFS data were fitted with the theoretical EXAFS function using the FEFFIT (2.52) program.[34] E_o is one of the fitting parameters in the FEFFIT program. Initially, it was taken as the energy corresponding to the first inflection point in the derivative spectra of the individual compound. For Pt metal, it is found to be 11561 eV within the error of 1 eV. After fitting, the final values of E_o obtained are 11562.9, 11571.9, and 11573.4 eV for Pt metal, Pt acetyl acetonate, and PtO_2, respectively. The goodness of fit has been judged by means of χ^2, reduced χ^2, and R factor discussed elsewhere.[35,36] From this analysis structural parameters such as coordination numbers (N), bond distance (R), and Debye−Waller factor (σ) have been calculated.

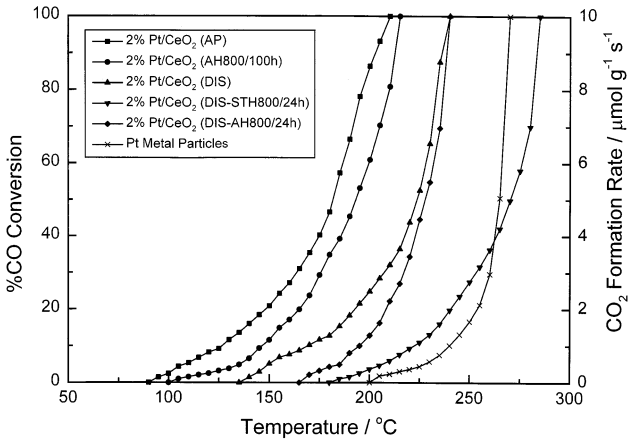

Figure 1. %CO conversion and corresponding rates for CO + O_2 reaction on as-prepared (AP) and heat-treated (AH800/100h) combustion-synthesized 2% Pt/CeO_2; as-prepared (DIS), sealed tube heated (DIS-STH800/24h), and air-heated (DIS-AH800/24h) 2% Pt/CeO_2 (dispersed); Pt metal particles.

Results

Catalytic Test. CO oxidation by O_2 was carried out over as-prepared and heat-treated 2% Pt/CeO_2 at a gas hourly space velocity (GHSV) of 43000 h^{-1}. Percentage of CO conversion and CO_2 formation rates over these catalysts as a function of temperature is presented in Figure 1. The light-off temperatures (temperature at 50% conversion) are 180 and 190 °C for as-prepared and heat-treated 2% Pt/CeO_2, respectively. In the same figure, percentage of CO conversion over fine Pt metal particles and as-prepared 2% Pt/CeO_2 (dispersed) and the same sample heat-treated in air and in an evacuated sealed tube are given for comparison. The reaction conditions, gas flow rates, amount of catalyst, and Pt loading were the same as those for the combustion-synthesized 2% Pt/CeO_2 catalysts. Clearly, CO oxidation occurs at a much lower temperature over combustion-synthesized 2% Pt/CeO_2 compared to 2% Pt/CeO_2 (dispersed) and fine Pt metal particles. Catalytic activity of sealed tube heated 2% Pt/CeO_2 (dispersed) is similar to that of Pt metal particles. Activation energies [from Arrhenius plot of ln(rate) vs $1/T$] of CO oxidation are 44, 52, and 106 kJ mol^{-1} over combustion-synthesized 2% Pt/CeO_2, 2% Pt/CeO_2 (dispersed), and fine Pt metal particles, respectively. There is a slight decrease in the catalytic activity of combustion-synthesized catalyst after heating it at 800 °C for 100 h, but it is still far higher than Pt/CeO_2 (dispersed) and Pt metal particles. Similarly, CO + O_2 reaction occurs at a much lower temperature over combustion-synthesized 1% Pt/CeO_2 compared to Pt metal particles of the same concentra-

(30) Stern, E. A.; Kim, K. *Phys. Rev. B* **1981**, *23*, 3781.
(31) Newville, M.; Līviņš, P.; Yacoby, Y.; Rehr, J. J.; Stern, E. A. *Phys. Rev. B* **1993**, *47*, 14126.
(32) Pearson, W. P. In *Handbook of Lattice Spacings and Structures of Metals and Alloys*; Pergamon: New York, 1958.
(33) Zabinsky, S. I.; Rehr, J. J.; Ankudinov, A.; Albers, R. C.; Eller, M. J. *Phys. Rev. B* **1995**, *52*, 2996.
(34) Stern, E. A.; Newville, M.; Ravel, B.; Yacoby, Y.; Haskel, D. *Physica B* **1995**, *208* and *209*, 117.
(35) Press, W. H.; Teulosky, S. A.; Vetterling, W. T.; Flannery, B. P. In *Numerical Recipies*; Cambridge University Press: New York, 1992.
(36) Bevington, P. R. In *Data Reduction and Error Analysis for Physical Sciences*; McGraw-Hill: New York, 1969.

tion. The catalytic activity thus depends on the structure of Pt/CeO_2 catalyst. The chemical environment of Pt in combustion-synthesized Pt/CeO_2 is different from that of Pt in 2% Pt/CeO_2 (dispersed) and fine Pt metal particles. Therefore, it is important to investigate the structure of Pt/CeO_2 catalyst synthesized by the combustion method.

XRD Studies. A careful XRD study was undertaken to see if platinum ions were incorporated into a CeO_2 matrix in Pt/CeO_2 catalysts. Observed, calculated, and difference XRD patterns of as-prepared 1% Pt/CeO_2 are shown in Figure 2a. Rietveld refinements are carried out by varying 19 parameters such as overall scale factor, background parameters, unit cell, shape, and isotropic thermal parameters, and oxygen occupancy. The diffraction lines are indexed to fluorite structure ($Fm3m$). In 1% Pt/CeO_2, the R_{Bragg}, R_F, and R_P values are 1.31, 0.819, and 3.4%, respectively. The lattice parameter "a" is 5.4105 (2) Å. Pure CeO_2 was also refined and R_{Bragg}, R_F, and R_P are 0.91, 0.70, and 4.4%, respectively. The a value for pure CeO_2 is 5.4113 (3) Å. Total oxygen in 1% Pt/CeO_2 is 1.883 and that in pure CeO_2 is 1.934. The quality of X-ray data is to be considered good from an excellent signal to noise ratio. The fitting is good as seen from R factor values. In 1% Pt/CeO_2, no impurity lines are seen corresponding to any of the platinum oxides. Even though the X-ray scattering factor of oxygen is low compared to that of cerium, absolute oxygen content obtained from the refinement can give us the trend in the variation of oxygen content. A decrease of oxygen content from 1.934 in pure CeO_2 to 1.883 in 1% Pt/CeO_2 is significant. There is a decrease in the lattice parameter in 1% Pt/CeO_2 compared to that in pure CeO_2, but it is small. In Figure 2a, a small broad hump at $2\theta = 39.8°$ due to Pt(111) can be seen in the pattern when the region is exploded, indicating the presence of a trace amount of Pt metal particles. To examine the expected Pt(111) peak intensity in the XRD pattern, polyol-synthesized Pt particles (6−7 nm size) was physically mixed with pure CeO_2 to a 1 at. % Pt level and its XRD pattern was recorded. The XRD patterns of 1% Pt/CeO_2 catalyst and 1% Pt + CeO_2 were blown up to the same scale with reference to the CeO_2(111) peak. The intensity ratio of Pt(111) in 1% Pt/CeO_2 to that in a 1% Pt + CeO_2 physical mixture is 0.08. Thus, XRD studies show that at least 0.92 at. % of the platinum taken in the preparation of 1 at. % Pt/CeO_2 is incorporated in the CeO_2 lattice. Therefore, Rietveld analysis does indicate the possible substitution of platinum ions in Ce^{4+} sites in a CeO_2 matrix.

Observed, calculated, and difference XRD patterns of heat-treated 1% Pt/CeO_2 are presented in Figure 2b. In heat-treated 1% Pt/CeO_2, the R_{Bragg}, R_F, and R_P values are 0.572, 0.489, and 3.84%, respectively. The lattice parameter a is 5.4108(1) Å. Total oxygen content is 1.889. No significant variation in the lattice parameters and oxygen content is observed on heating at 800 °C for 100 h. However, immediate impression from the comparison of parts a and b in Figure 2 would be that the Pt metal intensity at $2\theta = 39.8°$ has gone up on heating. But a very broad peak due to Pt(111) is detected in an as-prepared sample, whereas it is sharp on heat treatment. Therefore, the relative intensity of Pt(111) with respect to CeO_2(111) is more important in determining the amount of Pt separated into Pt metal. Hence, the ratio of area under the peaks of Pt(111) to CeO_2(111) in both as-prepared and heat-treated samples was measured. The ratio is 0.046 in an as-prepared sample, whereas it is 0.035 in a heat-treated sample, indicating that the metal concentration in the heat-treated sample is decreased. Further, a broad Pt(111) peak in the as-prepared sample shows that the size of Pt particles is smaller than that in the heat-treated sample.

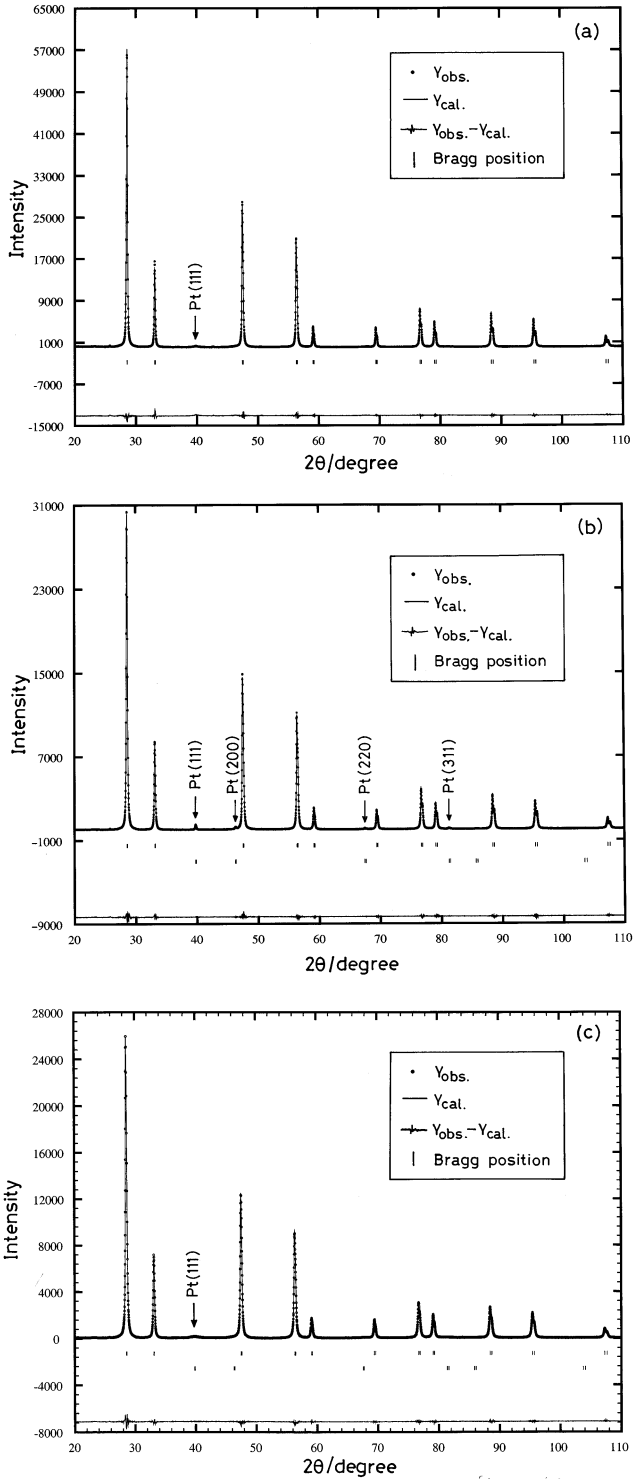

Figure 2. Observed, calculated, and difference XRD patterns of (a) as-prepared 1% Pt/CeO_2, (b) 1% Pt/CeO_2 heated at 800 °C for 100 h, and (c) as-prepared 2% Pt/CeO_2.

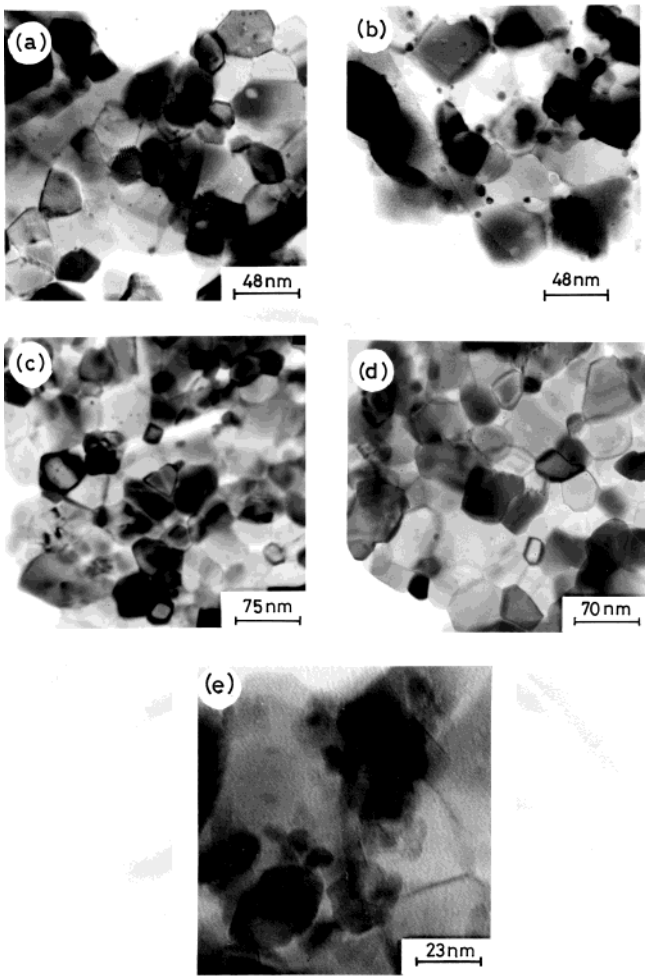

Figure 3. TEM of as-prepared (a) 1% Pt/CeO_2 and (b) 2% Pt/CeO_2 and heat-treated (800 °C for 100 h) (c) 1% Pt/CeO_2 and (d) 2% Pt/CeO_2 and (e) as-prepared 2% Pt/CeO_2 (dispersed).

Similarly, Rietveld analysis of 2% Pt/CeO_2 data was also carried out. In Figure 2c observed, calculated, and difference XRD patterns of as-prepared 2% Pt/CeO_2 are shown. Here also a broad hump at 39.8° due to Pt(111) is obtained along with CeO_2 peaks. Lattice parameter *a* is 5.4106 (3) Å with an oxygen occupancy of 1.921. R_{Bragg}, R_F, and R_P values are 0.966, 0.586, and 4.43%, respectively. The area under a Pt(111) to CeO_2(111) ratio is 0.048, which is the same with 1% Pt/CeO_2. On heating, the Pt(111) peak grew sharper but still the Pt(111)/CeO_2(111) intensity ratio is 0.047. Further, lattice parameter *a* is 5.4104 (1) Å and oxygen occupancy is 1.844 in a heat-treated sample. R_{Bragg}, R_F, and R_P values are 0.624, 0.455, and 4.14%, respectively. The peaks due to PtO or PtO_2 could not be detected to the extent of Pt metal in 2% Pt/CeO_2. Even in 4% Pt/CeO_2, PtO or PtO_2 phases have not been detected.

XRD pattern of 2% Pt/CeO_2 (dispersed) shows that the Pt(111) to CeO_2(111) area intensity ratio is 0.08, indicating that the Pt metal content is higher than that in the combustion-synthesized material. Sealed tube heated 2% Pt/CeO_2 (dispersed) shows more Pt metal concentration in relation to air-heated 2% Pt/CeO_2 (dispersed).

TEM Studies. TEM images of as-prepared and heat-treated 1 and 2% Pt/CeO_2 are given in Figure 3. Average sizes of CeO_2 crystallites are in the range 25−32 nm. The morphology of CeO_2 crystallites is cubic. Very few Pt particles can be seen on CeO_2 crystallites in a 1% Pt/CeO_2 catalyst [Figure 3a]. The number of Pt particles are higher in the case of 2% Pt/CeO_2 [Figure 3b]. In contrast, a large number of nanosize fine Pt metal particles can be dispersed on α-Al_2O_3 by the solution combustion method.[37] The average sizes of Pt particles on α-Al_2O_3 are 7−10 nm, whereas Pt particles detectable in 1% Pt/CeO_2 are smaller in size (4−5 nm). Thus, TEM studies demonstrate that over as-prepared 1% Pt/CeO_2 an extremely small amount of Pt is present as metal particles and the rest are dispersed as atoms or ions that could not be detected. TEM images of heat-treated 1 and 2% Pt/CeO_2 are shown in Figure 3c,d. There is about a 35−40% increase in grain size of CeO_2 crystallites on prolonged heat treatment. It is important to note from the TEM images that there is a decrease in the Pt metal particle density on heating. Smaller Pt particles might have grown bigger in size due to heat treatment. This observation is in full agreement with XRD studies.

TEM of Pt/CeO_2 (dispersed) was also studied as shown in Figure 3e. The average sizes of CeO_2 crystallites are in the range 25−35 nm. TEM image shows a greater number of Pt particles and also the number of Pt particles per unit area is higher than that in combustion-synthesized Pt/CeO_2.

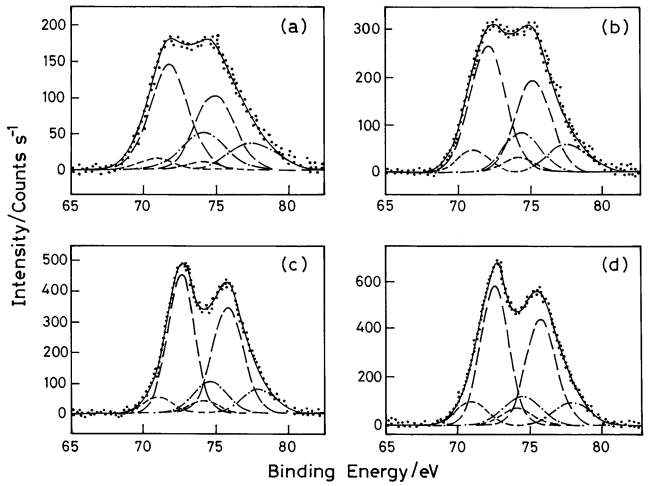

Figure 4. XPS of core level region of Pt in as-prepared (a) 1% Pt/CeO_2 and (b) 2% Pt/CeO_2 and heat-treated (c) 1% Pt/CeO_2 and (d) 2% Pt/CeO_2 at 800 °C for 100 h.

XPS Studies. XPS of the Pt(4f) core level region in as-prepared and heat-treated 1% Pt/CeO_2 and 2% Pt/CeO_2 are given in Figure 4. The Pt(4f) region shows peaks due to multiple oxidation states in Pt/CeO_2 samples. Pt($4f_{7/2,5/2}$) peaks in Pt/CeO_2 catalysts were deconvoluted into three sets of spin−orbit doublet. Accordingly, Pt($4f_{7/2,5/2}$) peaks at 71.0, 74.2; 71.9, 75.1; and 74.3, 77.5 eV could be assigned to Pt metal, Pt^{2+}, and Pt^{4+}, respectively [Figure 4a].[2,38] Here, Pt is found to be dispersed mostly in +2 (72%) and +4 (21%) oxidation states on CeO_2 crystallites with only 7% Pt present as Pt^0 state. If the curves are resolved into only two sets of Pt(4f) peaks for Pt^{2+} and Pt^{4+}, full width at half maximum (fwhm) of Pt^{2+} peaks becomes too high

(37) Bera, P.; Patil, K. C.; Jayaram, V.; Hegde, M. S.; Subbanna, G. N. *J. Mater. Chem.* **1999**, *9*, 1801.
(38) Shyu, J. Z.; Otto, K. *J. Catal.* **1989**, *115*, 16.

Table 1. Binding Energies, Relative Intensities, and fwhm's of Different Platinum Species as Observed from Pt(4f) Spectra of As-Prepared Pt/CeO_2 Catalysts with Various Pt Concentrations

catalyst	species	binding energy of $4f_{7/2}$ (eV)	relative intensity (%)	fwhm (eV)
1% Pt/CeO_2	Pt^0	71.0	7	2.6
	Pt^{2+}	71.9	72	3.0
	Pt^{4+}	74.3	21	3.3
2% Pt/CeO_2	Pt^0	71.0	12	2.4
	Pt^{2+}	72.1	69	2.6
	Pt^{4+}	74.4	19	3.3
3% Pt/CeO_2	Pt^0	71.0	18	2.4
	Pt^{2+}	71.5	63	3.1
	Pt^{4+}	74.4	19	3.3
4% Pt/CeO_2	Pt^0	70.8	22	2.4
	Pt^{2+}	71.6	60	2.7
	Pt^{4+}	74.3	18	3.2
5% Pt/CeO_2	Pt^0	70.9	29	2.4
	Pt^{2+}	71.9	52	2.7
	Pt^{4+}	74.5	19	3.4

Table 2. Binding Energies, Relative Intensities, and fwhm's of Different Platinum Species as Observed from Pt(4f) Spectra of Pt/CeO_2 Catalysts with Various Pt Concentrations Heated at 800 °C for 100 h

catalyst	species	binding energy of $4f_{7/2}$ (eV)	relative intensity (%)	fwhm (eV)
1% Pt/CeO_2	Pt^0	71.0	9	2.7
	Pt^{2+}	72.9	76	2.8
	Pt^{4+}	74.6	15	3.2
2% Pt/CeO_2	Pt^0	71.1	13	2.2
	Pt^{2+}	72.8	71	2.4
	Pt^{4+}	74.9	16	3.5
3% Pt/CeO_2	Pt^0	71.1	20	1.9
	Pt^{2+}	72.8	65	2.7
	Pt^{4+}	74.9	15	3.3
4% Pt/CeO_2	Pt^0	71.1	23	2.7
	Pt^{2+}	72.6	61	2.9
	Pt^{4+}	75.2	15	3.4
5% Pt/CeO_2	Pt^0	71.1	29	2.4
	Pt^{2+}	72.5	57	2.9
	Pt^{4+}	74.6	14	3.3

(3.6 eV), which is nonphysical. Therefore, a trace amount of Pt metal (Pt^0) is taken into account in XPS analysis. This observation agrees well with the XRD and TEM studies. Similarly, Pt($4f_{7/2}$) peaks at 71.0, 72.1, and 74.4 eV in 2% Pt/CeO_2 could be attributed to Pt metal, Pt^{2+}, and Pt^{4+}, respectively. For 4% Pt/CeO_2, the amount of Pt metal is higher than 1 and 2% Pt/CeO_2. In the same figure, Pt(4f) core levels in 1 and 2% Pt/CeO_2 samples heated at 800 °C are shown. There are significant changes in the Pt(4f) spectra of heat-treated samples as seen from Figure 4c,d. The spectra could also be deconvoluted into three components of Pt(4f). On prolonged heating, an increase in the Pt^{2+} state at the expense of the Pt^{4+} state is observed. The Pt^0 metal concentration is about the same. Further, there is an increase in the binding energies of the Pt^{2+}(4f) peak from 71.9 ± 0.2 to 72.8 ± 0.2 eV. The binding energies, relative intensities, and fwhm's of different platinum species as observed from Pt(4f) spectra of as-prepared and heat-treated Pt/CeO_2 catalysts with various Pt concentrations are summarized in Tables 1 and 2, respectively.

Pt(4f) regions of Pt metal particles, sealed tube heated, and air-heated 2% Pt/CeO_2 (dispersed) are shown in Figure 5. In Pt metal particles, $4f_{7/2,5/2}$ peaks are observed at 71.1 and 74.3 eV, respectively, with a

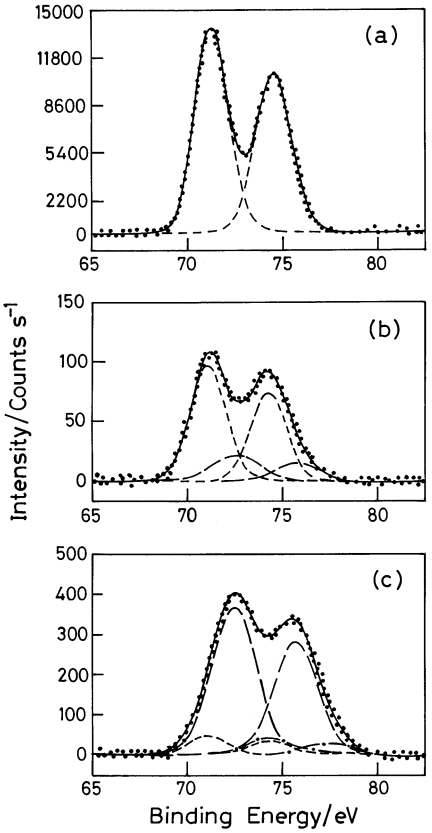

Figure 5. XPS of core level region of Pt in (a) Pt metal particles, (b) sealed tube heated (800 °C for 24 h) 2% Pt/CeO_2 (dispersed), and (c) air-heated (800 °C for 24 h) 2% Pt/CeO_2 (dispersed).

Table 3. Binding Energies, Relative Intensities, and fwhm's of Different Platinum Species as Observed from Pt(4f) Spectra of Pt Metal Particles and Sealed Tube Heated and Air-Heated 2% Pt/CeO_2 (dispersed) Catalysts at 800 °C for 24 h

catalyst	species	binding energy of $4f_{7/2}$ (eV)	relative intensity (%)	fwhm (eV)
Pt metal particles	Pt^0	71.1	100	2.2
sealed tube heated	Pt^0	71.1	80	2.2
2% Pt/CeO_2	Pt^{2+}	72.4	20	2.7
air-heated	Pt^0	71.1	8	2.3
2% Pt/CeO_2	Pt^{2+}	72.4	83	2.7
	Pt^{4+}	74.5	9	3.1

fwhm of 2.2 eV. XPS of sealed tube heated 2% Pt/CeO_2 (dispersed) could be resolved into two sets of spin−orbit doublet. Accordingly, Pt($4f_{7/2,5/2}$) peaks at 71.1, 74.3 and 72.4, 75.7 eV could be assigned to Pt^0 and Pt^{2+}, respectively [Figure 5b]. Here, Pt is found to be dispersed mostly (80%) in the metallic state on CeO_2 crystallites with about 20% Pt in the Pt^{2+} state. In the sample after air heating, Pt(4f) peaks are observed at 71.1, 74.3; 72.4, 75.6; and 74.5, 77.7 eV corresponding to Pt^0, Pt^{2+}, and Pt^{4+}, respectively [Figure 5c]. The binding energies, relative intensities, and fwhm's of different platinum species as observed from Pt(4f) spectra of Pt metal particles, as-prepared, sealed tube heated, and air-heated Pt/CeO_2 catalysts with various Pt concentrations are summarized in Table 3.

In Figure 6, Ce(3d) peaks obtained from Pt/CeO_2 samples at different conditions are shown. The spectra with satellite features (marked in the figures) cor-

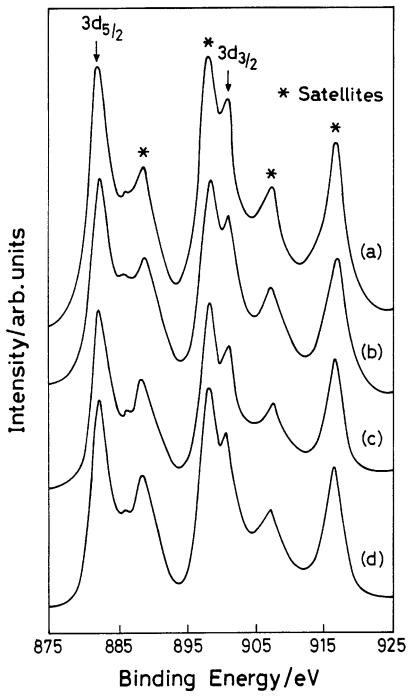

Figure 6. XPS core level region of Ce(3d) in as-prepared 1% Pt/CeO_2 and 2% Pt/CeO_2 and heat-treated (800 °C for 100 h) 1% Pt/CeO_2 and 2% Pt/CeO_2.

respond to CeO_2 with Ce in the +4 oxidation state.[2,39] There may be a trace component of reduced CeO_2 in the spectrum due to Ce^{3+} as obtained in UHV (10^{-9} Torr) conditions. An increase in the intensities of Ce(3d) peaks along with satellites is observed on heat treatment. An O(1s) peak is seen at 530 ± 0.2 eV and no significant change in the peak position of O(1s) is noticed on heat treatment.

XRD, TEM, XPS, and heat-treatment studies on combustion-synthesized 1 and 2% Pt/CeO_2 show that Pt is largely dispersed as ions over nanosize CeO_2 crystallites. CO + O_2 reaction occurs at a much lower temperature compared to Pt/CeO_2 (dispersed) and Pt metal particles. Therefore, EXAFS study was carried out on as-prepared as well as heat-treated combustion-synthesized Pt/CeO_2 samples to understand the structure.

EXAFS Studies. The normalized XANES spectra of model compounds, Pt metal, Pt acetyl acetonate (Pt-acac), PtO_2, and catalyst samples of as-prepared 2% Pt/CeO_2 and heat-treated 1 and 2% Pt/CeO_2 are presented in Figure 7. The edge energy as determined from the first maxima in the derivative spectra, for Pt metal is found to be 11561.0 eV. It is shifted to 11561.9 and 11562.9 eV for Pt-acac and PtO_2, respectively. Another difference in the XANES spectra of the model compounds is in the intensity and sharpness of the first intense maxima or the white line. The intensity of the white line reflects the unoccupancy of Pt(5d) orbital because this maxima corresponds to electron transition from 2p to 5d of the Pt atom. Thus, the intensity is related to the oxidation state of Pt in the model compound.[40−42] In the case of catalyst samples, with the

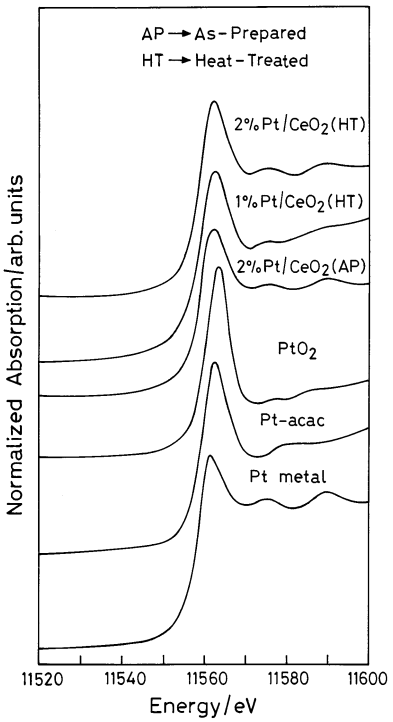

Figure 7. Normalized XANES spectra at Pt L_{III}-edge of PtO_2, Pt-acac, Pt metal, as-prepared 2% Pt/CeO_2 and heat-treated 1 and 2% Pt/CeO_2.

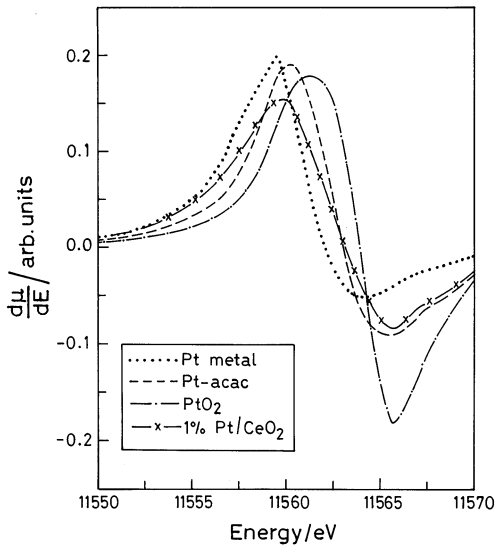

Figure 8. Derivative spectra of Pt metal, Pt-acac, PtO_2, and heat-treated 1% Pt/CeO_2.

exception of the heat-treated 1% Pt/CeO_2, the value of edge energy is found to be around 11560.9 eV, indicating the presence of Pt metal phase. For heat-treated 1% Pt/CeO_2, the value of edge energy is 11561.5 eV, which is the average of edge energies in Pt metal and Pt-acac. This is very clearly seen in Figure 8, which shows the derivative spectra of the model compounds along with heat-treated 1% Pt/CeO_2. It must, however, be noted that the intensity of the white line in all the catalyst samples is higher than that in Pt metal, indicating part of the Pt atom exists in oxidized states. The normalized EXAFS spectra of Pt metal, PtO_2, and catalysts are

(39) Sarma, D. D.; Hegde, M. S.; Rao, C. N. R. *J. Chem. Soc., Faraday Trans. 2* **1981** *77*, 1509.
(40) Cracium, R.; Shereck, B.; Gorte, R. J. *Catal. Lett.* **1998**, *51*, 149.
(41) Kepinski, L.; Wolcyrz, M. *Appl. Catal. A* **1997**, *150*, 197.
(42) Bensalem, A.; Muller, J.-C.; Tessier, D.; Bozon-Verduraz, F. *J. Chem. Soc., Faraday Trans.* **1996**, *92*, 3233.

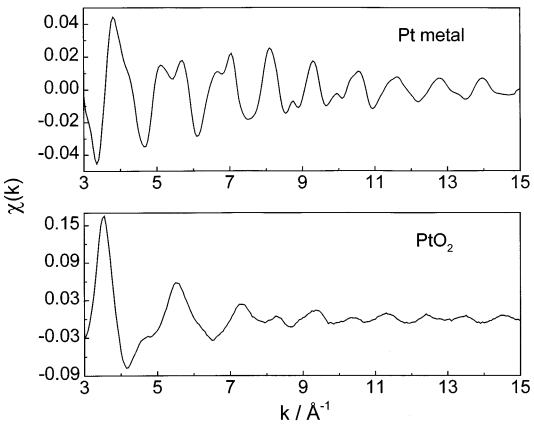

Figure 9. EXAFS functions of Pt metal and PtO_2.

presented in Figures 9 and 10, respectively. The EXAFS spectra of both the as-prepared and heat-treated 2 and 4% Pt/CeO_2 show some similarities to EXAFS of Pt metal. However, there are some distinct differences in both the as-prepared and heat-treated 1% Pt/CeO_2. The noticeable difference is the double-peak structure between 5 and 6 $Å^{-1}$ in both the samples.

Figure 11 shows the k^3 weighted Fourier transform (FT) of the EXAFS spectra for Pt metal and PtO_2 along with their inverse transforms. The Fourier transforms are not corrected for phase shift and hence the peaks are shifted to lower R values. The values of bond distance quoted in the text and table are, however, corrected for phase shift. For Pt metal foil, the Pt−Pt scattering peak is seen at 2.76 Å. In addition to it, a small peak on the lower R side of the main peak can be seen. This is caused by both the k-dependent behavior of backscattering amplitude and nonlinearity in the phase shift function.[43] Pt−O correlation in PtO_2 appears at about 1.99 Å and a Pt−Pt correlation is observed at an average distance of 3.15 Å. The values of bond distance, coordination number, and Debye−Waller factors obtained from fitting the EXAFS data in the R range 1−4 Å are presented in Table 4. These values agree well with the structural data of Pt and PtO_2. EXAFS of PtO is computed using the crystallographic data in ATOMS and FEFF 6.0. Pt−O correlation with 4 coordination number is observed at 2.14 Å in the first shell. There are two Pt−Pt correlations having 2 and 4 coordination numbers at 2.67 and 3.04 Å, respectively. The EXAFS parameters obtained from the computation of crystallographic data of PtO are also given in Table 4. Debye−Waller factors and precision from PtO data analysis cannot be obtained as it is computed data.

Table 4. Structural Parameters of Pt Metal, PtO_2, and PtO (Computed) Obtained from EXAFS Analysis

samples	shell	N	R (Å)	σ^2 ($Å^{-2}$)
Pt metal	Pt−Pt	12.00	2.758 ± 0.004	0.009 ± 0.001
		6.00	3.901 ± 0.005	0.013 ± 0.003
		48.00	4.138 ± 0.005	0.016 ± 0.003
		24.00	4.778 ± 0.006	0.015 ± 0.002
PtO_2	Pt−O	5.6 ± 0.2	1.989 ± 0.004	0.002 ± 0.001
	Pt−Pt	3.7 ± 0.2	3.153 ± 0.002	0.006 ± 0.001
	Pt−Pt	7.6 ± 0.4	3.556 ± 0.006	0.014 ± 0.008
	Pt−O	4.5 ± 0.6	3.695 ± 0.006	0.005 ± 0.002
PtO (computed)	Pt−O	4.00	2.145	
	Pt−Pt	2.00	2.670	
	Pt−Pt	4.00	3.040	
	Pt−O	8.00	3.428	

Figure 12 shows the k^3 weighted FT spectra of as-prepared and heat-treated 1, 2, and 4% Pt/CeO_2 catalysts. As above, FT spectra are not corrected for phase shift but the values in the text and the tables are phase-corrected. In all these samples, a correlation at about 2.0 Å is seen, which is absent in Pt metal. This is attributed to the Pt−O bond. The second correlation at 2.31 Å does not match any correlation of PtO_2 or PtO. The third broad peak distinctly consists of two correlations, one at 2.78 Å matching the Pt−Pt correlation in Pt metal and another at 2.97 Å. In the case of 1% Pt/CeO_2, the peak at 2.78 Å due to Pt−Pt is of lower intensity than the other peak, whereas in the 2 and 4% Pt/CeO_2, the Pt−Pt correlation at 2.78 Å is more intense than the other. There is another small correlation at

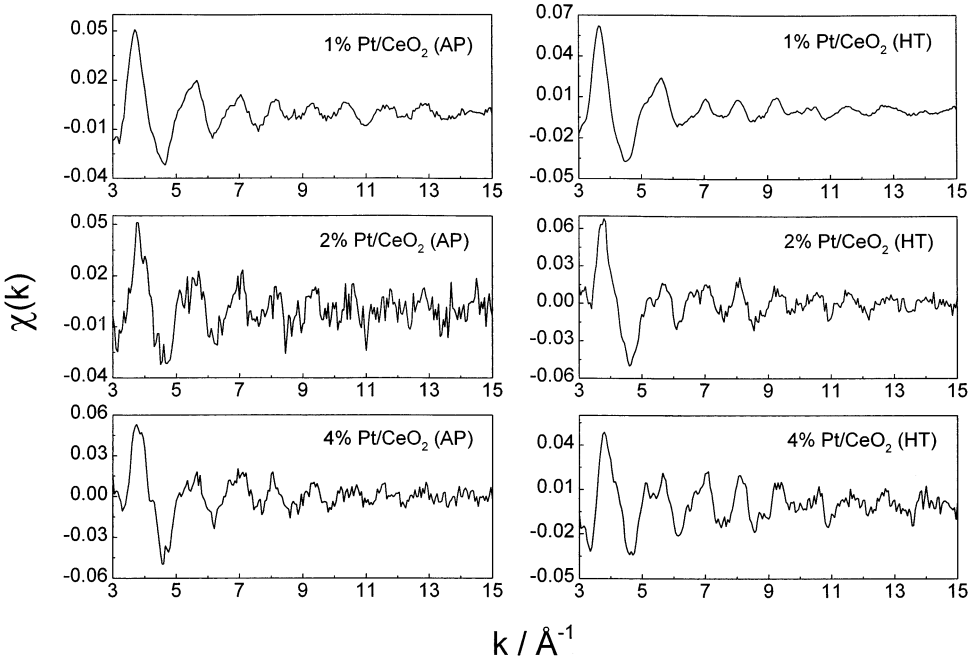

Figure 10. EXAFS functions of as-preapared and heat-treated 1, 2, and 4% Pt/CeO_2 [AP = as-prepared, HT = heat-treated].

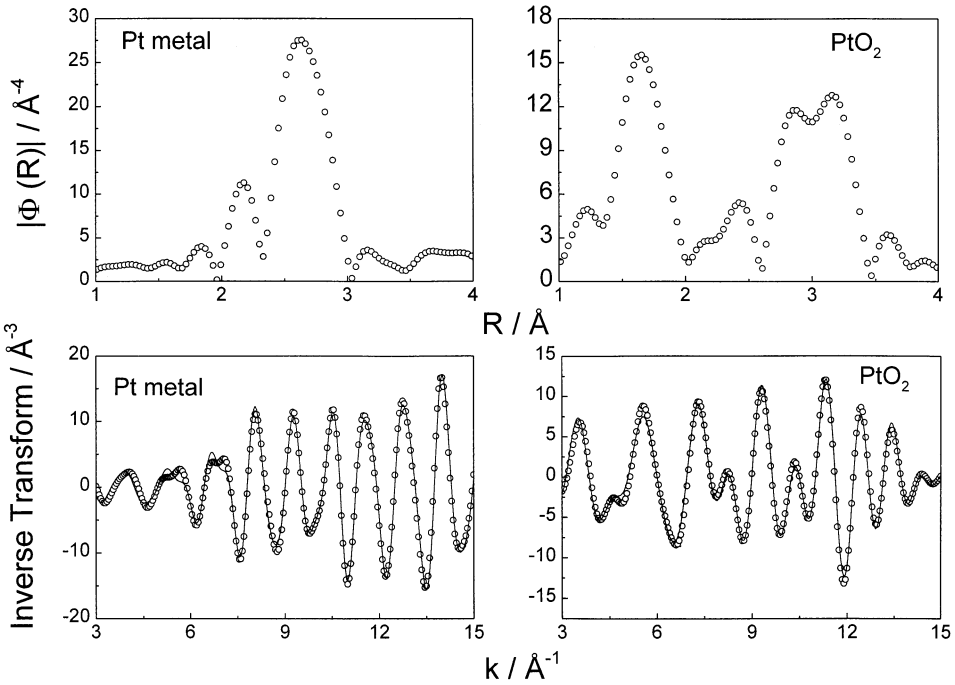

Figure 11. Fourier transforms and inverse transforms of Pt metal and PtO_2.

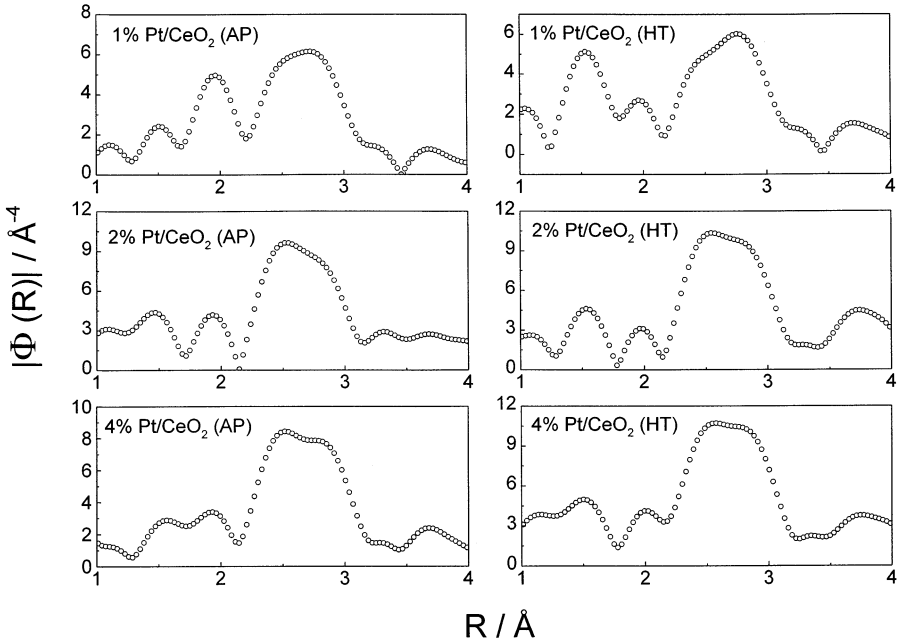

Figure 12. Fourier transforms of as-prepared and heat-treated 1, 2, and 4% Pt/CeO_2 [AP = as-prepared, HT = heat-treated].

3.28 Å, which is absent in either Pt metal or PtO_2. It is also absent in the simulated data for PtO structure. Therefore, Pt/CeO_2 catalysts contain Pt metal and Pt in the ionic phase, which is different from PtO and PtO_2. From the XPS studies of both as-prepared and heat-treated 1% Pt/CeO_2, Pt is found to be present mostly as Pt ions (Pt^{2+}, 72%, and Pt^{4+}, 21%, in 1% Pt/CeO_2). Less than 10% Pt in the metallic phase has been detected in both cases. XRD studies show that Pt metal is present to the extent of 5−8%. Since we do not see any of the Pt oxide phases even to the extent of Pt metal phase, we assume that Pt ions occupy the Ce^{4+} sites in the CeO_2 matrix. Therefore, EXAFS data were fitted with Pt−O, Pt−Pt, and Pt−Ce correlations of $Ce_{1-x}Pt_xO_{2-\delta}$ type solid solution phase along with the first two correlations of Pt metal. The fitted parameters obtained for as-prepared and heat-treated catalysts are listed in Tables 5 and 6, respectively. Pt−Pt correlations of the metal phase at 2.78 and 3.92 Å agree well with the 12- and 6-coordinated shells at 2.76 and 3.90 Å of Pt metal, respectively. It must be noted that the decrease in coordination number in the catalysts indicates the smaller particle size and higher dispersion on the surface. In solid solution phase, Pt has about ∼1.5 oxygen atoms in the first coordination in the as-prepared catalysts, which increases to ∼2.0 in the heat-treated samples. If Pt ions are substituted for Ce^{4+} sites,

(43) van Zon, J. B. A. D.; Koningsberger, D. C.; van't Blik, H. F. J.; Prins, R.; Sayers, D. E. *J. Chem. Phys.* **1984**, *80*, 3914.

Table 5. Structural Parameters for As-Prepared Pt/CeO_2 Catalysts Obtained from EXAFS Analysis

catalysts	shell	N	R (Å)	σ^2 (Å^{-2})
1% Pt/CeO_2	[a]Pt−Pt	5.8 ± 0.6	2.779 ± 0.006	0.005 ± 0.001
	Pt−O	1.3 ± 0.3	1.983 ± 0.004	0.004 ± 0.001
	Pt−Pt	4.6 ± 0.3	2.977 ± 0.005	0.027 ± 0.003
	Pt−Ce	2.6 ± 0.3	3.274 ± 0.004	0.016 ± 0.002
	[a]Pt−Pt	2.2 ± 0.2	3.921 ± 0.004	0.006 ± 0.001
2% Pt/CeO_2	[a]Pt−Pt	7.7 ± 0.8	2.779 ± 0.006	0.005 ± 0.001
	Pt−O	1.6 ± 0.2	2.011 ± 0.005	0.004 ± 0.001
	Pt−Pt	3.8 ± 0.4	2.972 ± 0.005	0.012 ± 0.002
	Pt−Ce	3.2 ± 0.3	3.284 ± 0.003	0.026 ± 0.003
	[a]Pt−Pt	3.3 ± 0.4	3.933 ± 0.006	0.006 ± 0.001
4% Pt/CeO_2	[a]Pt−Pt	7.3 ± 0.7	2.784 ± 0.004	0.005 ± 0.001
	Pt−O	1.4 ± 0.2	2.044 ± 0.003	0.004 ± 0.001
	Pt−Pt	5.9 ± 0.6	2.972 ± 0.004	0.021 ± 0.003
	Pt−Ce	1.1 ± 0.2	3.284 ± 0.002	0.025 ± 0.003
	[a]Pt−Pt	3.5 ± 0.3	3.913 ± 0.005	0.006 ± 0.001

[a]Pt−Pt coordination in the Pt metal phase.

Table 6. Structural Parameters for Pt/CeO_2 Catalysts Heat-Treated at 800 °C for 100 h Obtained from EXAFS Analysis

catalysts	shell	N	R (Å)	σ^2 (Å^{-2})
1% Pt/CeO_2	[a]Pt−Pt	5.2 ± 0.5	2.791 ± 0.004	0.005 ± 0.001
	Pt−O	2.3 ± 0.3	2.001 ± 0.003	0.005 ± 0.001
	Pt−Pt	2.4 ± 0.3	3.030 ± 0.005	0.015 ± 0.002
	Pt−Ce	5.6 ± 0.6	3.276 ± 0.005	0.023 ± 0.003
	[a]Pt−Pt	2.7 ± 0.3	3.920 ± 0.003	0.006 ± 0.001
2% Pt/CeO_2	[a]Pt−Pt	9.6 ± 0.9	2.787 ± 0.004	0.005 ± 0.001
	Pt−O	1.8 ± 0.2	1.986 ± 0.004	0.005 ± 0.001
	Pt−Pt	3.7 ± 0.4	2.959 ± 0.006	0.012 ± 0.002
	Pt−Ce	3.5 ± 0.4	3.285 ± 0.007	0.014 ± 0.002
	[a]Pt−Pt	6.0 ± 0.5	3.933 ± 0.004	0.006 ± 0.001
4% Pt/CeO_2	[a]Pt−Pt	9.7 ± 0.1	2.784 ± 0.003	0.005 ± 0.001
	Pt−O	1.7 ± 0.2	1.979 ± 0.003	0.005 ± 0.001
	Pt−Pt	5.4 ± 0.5	2.968 ± 0.005	0.022 ± 0.003
	Pt−Ce	3.2 ± 0.3	3.284 ± 0.005	0.017 ± 0.002
	[a]Pt−Pt	6.0 ± 0.6	3.946 ± 0.006	0.006 ± 0.001

[a]Pt−Pt coordination in the Pt metal phase.

the first coordination around Pt ion will be of oxide ions. In the case of pure CeO_2, Ce^{4+} ions will have 12 Ce^{4+} neighbors in bulk solid, but the surface Ce^{4+} ions will have only 8 Ce^{4+} ions. Due to substitution of Pt ions into Ce^{4+} sites, Pt ions will have correlations from Pt ion and Ce^{4+} ion in the second coordination. Because of different sizes of Pt ion and Ce^{4+} ion and also the ionic interaction between them, Pt−Pt and Pt−Ce correlations are obtained. However, the number of Pt ion and Ce^{4+} ions around Pt ion would depend on the extent of substitution. Accordingly, correlation of ∼2.0 Å in the catalyst is indeed due to the Pt−O bond and the bond distances at 2.97 and 3.28 Å can be attributed to Pt−Pt and Pt−Ce correlations, which are absent in Pt metal, PtO, and PtO_2. The total coordination number of these two correlations is around 7−8, which is expected if the surface Pt ions are substituted for Ce^{4+} ion in CeO_2. The second correlation at 2.31 Å can be largely accounted by the *k*-dependent backscattering amplitude and the nonlinearity of the phase shift function of the Pt−Pt correlation of the metal except in the case of the as prepared 1% Pt/CeO_2 catalyst.[43] The intensity of this peak is unusually high in the case of as-prepared 1% Pt/CeO_2. Several models were considered to fit this peak in the as-prepared 1% Pt/CeO_2. If we consider this peak to be due to Pt−O correlation arising from substitution of Pt^{4+} for Ce^{4+} in the CeO_2 matrix without any structural modification, the fit is very good but the coordination number and the Debye−Waller factor are negative, which is nonphysical. It is to be noted that the amplitude of this peak gradually decreases as Pt loading is increased and is further decreased in the corresponding heat-treated sample. The fitting based on the above model of the EXAFS data is quite good and is presented in the *k* space for the Fourier-filtered data in Figure 13.

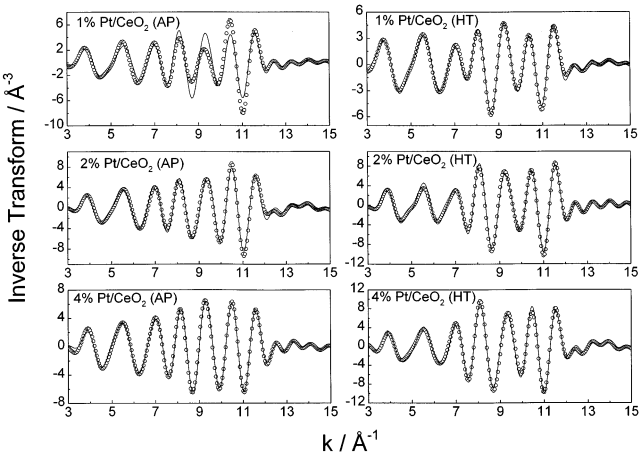

Figure 13. Inverse transforms of as-prepared and heat-treated 1, 2, and 4% Pt/CeO_2 [AP = as-prepared, HT = heat-treated].

Pt ion has 2 oxide ion coordination instead of 4 as Ce^{4+} ion on the surface is coordinated by 4 oxygen. Oxide ion vacancy can be created from the lower valent Pt ion substitution in place of Ce^{4+} ion. This is consistent with XPS studies where it is shown that Pt is mostly present in the +2 state. Therefore, in the solid solution model of $Ce_{1-x}Pt_xO_{2-\delta}$, the local chemical environment of Pt ion is modified due to the oxide ion vacancy. Comparing with PtO_2 or PtO, the Pt−Pt correlations at 3.15 Å in PtO_2 and 2.67 and 3.04 Å in PtO are absent in catalysts and instead a new Pt−Pt correlation at 2.97 Å is observed. This coupled with the Pt−Ce interaction at 3.28 Å clearly indicates that Pt ion in Pt/CeO_2 catalyst is different from that in PtO or PtO_2. The Pt−O−Ce correlation obtained at 3.28 Å needs to be accounted in the model. Ce^{4+}−O−Ce^{4+} at 3.82 Å is due to a Ce−O−Ce angle of 109.5°. If the angle decreases to 90° and assuming ionic radii of Pt^{2+} (0.80 Å), O^{2-} (1.4 Å), and Ce^{4+} (1.01 Å),[44] the Pt−Ce distance would be 3.21 Å, which is close to the observed value of 3.28 Å. Therefore, it is possible that the Pt−O−Ce angle is slightly higher than 90°. In our earlier studies, similar correlations for Pd−O−Ce and Cu−O−Ce at 3.31 and 3.15 Å, respectively, have been shown in Pd/CeO_2 and Cu/CeO_2 catalysts in the form of $Ce_{1-x}M_xO_{2-\delta}$ (M = Pd and Cu) solid solution phase.[45,46]

Discussion

In the present study, the solution combustion method provides CeO_2 supported Pt catalysts in a single step. In combustion-synthesized Pt/CeO_2, Pt should be sepa-

(44) Dickinson, S. K., Jr. In *Ionic, Covalent and Metallic Radii of the Chemical Elements*; Airforce Cambridge Research Laboratories, L. G. Hanscom Field: Bedford, MA, 1970.
(45) Priolkar, K. R.; Bera, P.; Sarode, P. R.; Hegde, M. S.; Emura, S.; Kumashiro, R.; Lalla, N. P. *Chem. Mater.* **2002**, *14*, 2120.
(46) Bera, P.; Priolkar, K. R.; Sarode, P. R.; Hegde, M. S.; Emura, S.; Kumashiro, R.; Lalla, N. P. *Chem. Mater.* **2002**, *14*, 3591.

rated either into Pt metal clusters or Pt oxides from oxide support or Pt ion should be incorporated in the CeO_2 lattice. If there is an ionic substitution of Pt^{2+} ions for Ce^{4+} sites in the CeO_2 lattice, an oxide ion vacancy should be created to maintain the charge neutrality due to lower valent ionic substitution. Rietveld analysis of Pt/CeO_2 shows the oxide ion vacancy and the structure could be refined to the solid solution phase of $Ce_{1-x}Pt_xO_{2-\delta}$. In the XRD pattern about 0.08 at. % Pt metal out of 1 at. % Pt is indeed detected. If any of the oxides of Pt are formed, even at a 0.08% level, it could have been detected in the XRD. Since PtO and PtO_2 phases could not be detected, formation of these phases can be ruled out. In heat-treated samples, relative Pt metal concentration decreases. This could be due to the formation of more $Ce_{1-x}Pt_xO_{2-\delta}$ solid solution phase while Pt reacts with CeO_2 in air. In the TEM also, very few Pt metal particles are seen in the heat-treated samples. An increase in the grain size of CeO_2 after heat treatment is also observed to the extent of 30%. In XPS studies, it is shown that about 0.07% Pt in 1% Pt/CeO_2 is in the metallic state and the rest are in Pt^{2+} (72%) and Pt^{4+} (21%) states. Even though, at 1 at. % Pt level, it is difficult to ascertain Pt ion substitution, high-resolution XRD studies presented here certainly indicate the substitution of Pt^{2+} in the Ce^{4+} site by way of a decrease in the lattice parameter and total lattice oxygen compared to pure CeO_2. This is further substantiated by the fact that PtO or PtO_2 phase could not be detected from any of the experimental techniques studied here. Therefore, it is clear from the XRD, TEM, and XPS studies that Pt is in +2 and +4 oxidation states in Pt/CeO_2 with a trace amount of metal.

EXAFS studies show that Pt stabilizes in its ionic state primarily substituted for surface Ce^{4+} ions in the form of $Ce_{1-x}Pt_xO_{2-\delta}$ solid solution. EXAFS data analysis clearly indicates a direct $-Pt^{2+}-O-Ce^{4+}-$ correlation at a distance of 3.28 Å. In pure CeO_2, the oxygen ions are tetrahedrally coordinated to Ce^{4+} ions, giving a Ce−O−Ce angle of 109.5° and Ce−Ce distance of 3.82 Å. Pt substitution in the Ce site must bring a slight modification to the local environment around Pt. The respective Pt−O, Pt−Pt, and Pt−Ce correlations obtained from EXAFS analysis are ∼2.0, 2.97, and 3.28 Å and a Pt−O−Ce bond angle of ∼90°. On heat treatment, there is a consistent increase in the coordination number of Pt−O and Pt−Ce correlations, indicating the formation of stable solid solution phase. This observation is substantiated by the observed shift in $Pt^{2+}(4f_{7/2})$ binding energy peaks from 71.9 to 72.9 eV in XPS of 1% Pt/CeO_2. A similar binding energy shift is also observed in 2−5% Pt/CeO_2 catalysts (see Tables 1 and 2). In the as-prepared 1% Pt/CeO_2 sample, the average coordination number of oxygen is 1.3, which increases to 2.3 on heat treatment. Thus, in the heat-treated Pt/CeO_2, effective charge on Pt would increase due to an increase in coordination number. Therefore, there is complete agreement between XPS and EXAFS studies. Further, oxide ion vacancy is largely around Pt ions. Thus, substitution of Pt^{2+} for Ce^{4+} in the CeO_2 matrix results in the formation of solid solution phase, $Ce_{1-x}Pt_xO_{2-\delta}$. The study has also clearly demonstrated the stability of Pt in ionic form, even at 800 °C for a long period of time.

Detailed structural studies show that in the combustion-synthesized Pt/CeO_2, Pt is dispersed as ion in the form of $Ce_{1-x}Pt_xO_{2-\delta}$. It has been observed that CO + O_2 reaction occurs at a much lower temperature over combustion-synthesized Pt/CeO_2 in comparison with Pt/CeO_2 (dispersed) and Pt metal particles. Since Pt is present as mostly in the +2 state in combustion-synthesized Pt/CeO_2, Pt^{2+} ions should be the active sites for CO adsorption in the CO + O_2 reaction. In our earlier study, it was shown that CO is indeed adsorbed on Pt/CeO_2 and the quantity of CO adsorbed is high compared to that of Pt metal dispersed on Al_2O_3.[28]

The catalytic activity of 2% Pt/CeO_2 (dispersed) correlates well with the presence of Pt largely in the +2 state. The possibility of formation of a PtO kind of layer on a nano-CeO_2 surface due to heat treatment in air could not be ruled out. Such a material would have lower Pt^{2+} dispersion on CeO_2. This could be explained from the observed $Pt(4f_{7/2})$ peak at 72.4 eV in the air-heated 2% Pt/CeO_2 (dispersed) versus 72.8 eV in the combustion-synthesized 2% Pt/CeO_2 heated in air. However, Pt metal in the absence of air does not seem to interact with CeO_2 which is confirmed from XPS study. In sealed tube heated Pt/CeO_2 (dispersed), Pt remains as a metal with $Pt(4f_{7/2})$ at 71.1 eV. The catalytic activity of sealed tube heated Pt/CeO_2 (dispersed) is similar to that of the Pt metal particle.

For a higher rate of CO conversion at a lower temperature in the combustion-synthesized Pt/CeO_2, a higher amount of CO adsorption and availability of dissociated oxygen are essential. While Pt^{2+} ions act as CO adsorption sites, additional oxygen adsorption would help achieve this. Oxide ion vacancy as demonstrated from both XRD and EXAFS studies would be the natural oxygen adsorption site. We suggest that oxide ion vacancy in CeO_2 created by Pt^{2+} ion substitution can become an oxygen adsorption/dissociation site. Therefore, low-temperature CO + O_2 reaction over combustion-synthesized Pt/CeO_2 is attributed to $Pt-CeO_2$ interaction in the form of $Ce_{1-x}Pt_xO_{2-\delta}$ solid solution having $-\square-Pt^{2+}-O-Ce^{4+}-$ kinds of linkages.

Conclusions

(a) Pt ions dispersed over CeO_2 crystallites of 25−32 nm have been synthesized by the combustion technique.

(b) Rietveld refinement confirms the formation of $Ce_{1-x}Pt_xO_{2-\delta}$ in Pt/CeO_2 and absence of platinum oxide phases.

(c) TEM studies show that very few Pt particles are present in the as-prepared catalysts, which are further decreased on heat treatment.

(d) XPS studies show that Pt is in +2 and +4 states in 1% Pt/CeO_2 with a small amount of metal and on heating Pt^{2+} is stabilized at the cost of Pt^{4+} ions.

(e) XANES of catalysts show the presence of ionic Pt species along with Pt metal.

(f) Oxide ion vacancies are created around Pt ions.

(g) EXAFS analysis shows bond distances at 2.0, 2.97, and 3.28 Å in Pt/CeO_2 catalysts corresponding to $Pt^{2+}-O$, $Pt^{2+}-O-Pt^{2+}$, and $Pt^{2+}-O-Ce^{4+}$ correlations.

(h) There is a metal−ceria interaction that leads to the formation of solid solution $Ce_{1-x}Pt_xO_{2-\delta}$ on the surface due to substitution of Pt^{2+} into Ce^{4+} sites.

(i) There is an increase in Pt^{2+} concentration due to heat treatment, indicating the increase in the extent of solid solution.

Acknowledgment. Indian authors gratefully acknowledge Department of Science and Technology (DST), Government of India, for financial support. Thanks are also due to the authorities of Japan Synchrotron Radiation Research Institute (SPring-8), Japan, for allotting beamtime at BL01B1 beamline (Proposal No. 2001A0376-Cx-np) and for local hospitality. The author A. Gayen is thankful to the Council of Scientific and Industrial Research (CSIR), Government of India, for the award of a research fellowship.

CM0204775